

Synthesis and characterization of a focused-beam transmitarray antenna at 300 GHz

Francesco Foglia Manzillo, Orestis Koutsos, Benjamin Fuchs, Ronan Sauleau, Antonio Clemente

▶ **To cite this version:**

Francesco Foglia Manzillo, Orestis Koutsos, Benjamin Fuchs, Ronan Sauleau, Antonio Clemente. Synthesis and characterization of a focused-beam transmitarray antenna at 300 GHz. EuCAP 2022 - the European Conference on Antennas and Propagation 2022, Mar 2022, Madrid, Spain. cea-03637057

HAL Id: cea-03637057

https://cea.hal.science/cea-03637057

Submitted on 11 Apr 2022

HAL is a multi-disciplinary open access archive for the deposit and dissemination of scientific research documents, whether they are published or not. The documents may come from teaching and research institutions in France or abroad, or from public or private research centers.

L'archive ouverte pluridisciplinaire **HAL**, est destinée au dépôt et à la diffusion de documents scientifiques de niveau recherche, publiés ou non, émanant des établissements d'enseignement et de recherche français ou étrangers, des laboratoires publics ou privés.

Synthesis and Characterization of a Focused-Beam Transmitarray Antenna at 300 GHz

Francesco Foglia Manzillo *, Orestis Koutsos *, Benjamin Fuchs †, Ronan Sauleau †, Antonio Clemente *
*CEA-Leti, Univ. Grenoble Alpes, F-38000 Grenoble, France
e-mail: {francesco.fogliamanzillo, orestis.koutsos, antonio.clemente}@cea.fr
†Univ Rennes, CNRS, Institut d'Électronique et des Technologies du numéRique (IETR), UMR 6164, 35000 Rennes, France

***Abstract*—This paper presents the synthesis, design and characterization of a centrosymmetric transmitarray antenna operating at 300 GHz. A broadside pencil beam with reduced sidelobe levels is obtained by fixing the illumination (i.e. feed and focal distance) and using a phase-only array synthesis procedure. The optimal aperture phase distribution is determined by means of an iterative convex optimization algorithm using semidefinite relaxation. Based on this distribution, a 400-element transmitarray comprising eight different unit cells is designed at 300 GHz, fabricated using low-cost printed circuit board technology and characterized. The measured results provide a first experimental validation of the synthesis approach.**

***Index Terms*—array synthesis, lens antennas, convex optimization, millimeter-wave antennas, sub-THz antennas.**

I. Introduction

High-gain and efficient antennas compatible with low-cost fabrication processes will be key for the dense deployment of high-capacity point-to-point links in next-generation wireless networks operating in the upper end of the millimeter-wave (mm-wave) spectrum (100-300 GHz) [1]. Given the severe path loss, the radiation patterns will have to fulfill strict envelopes to maximize the signal to noise ratio along the line of sight and minimize the power emitted in other directions. To this end, antenna architectures providing simple solutions for pattern shaping and effective synthesis methods are required. Phased array antennas offer the greatest flexibility for the control of the radiation pattern, but their loss and complexity make them unsuited for high-gain applications in this frequency range. Dielectric hemispherical lenses [2] are often preferred. However, the pattern optimization often leads to bulky lenses with complex shapes or multiple dielectric shells which are hard to accurately realize and lossy.

A transmitarray antenna (TAs) [3]–[10] can be seen as a flat lens, placed at a certain distance, typically in free space, from its feed. A planar array comprising multiple phase-shifting unit cells (UCs) realizes the lens. Thus, TAs inherit the advantages of dielectric lens antennas but are more efficient and suitable for planar multilayer fabrication processes, even beyond 100 GHz [4], [5]. The specifications on the TA size, gain and on the complexity of its primary source strongly limit the possibility to select a convenient amplitude taper for shaping the radiated beam. The use of lossy UCs for devising the amplitude distribution leads to a significant reduction of the aperture efficiency [6]. Therefore, efficient phase-only synthesis methods are necessary. Previous works mainly use either global optimization algorithms [7], [8] or alternating projection methods [9], [10]. The few shaped-beam TAs demonstrated at 300 GHz were mainly designed for near-field applications using UCs of variable thicknesses [10].

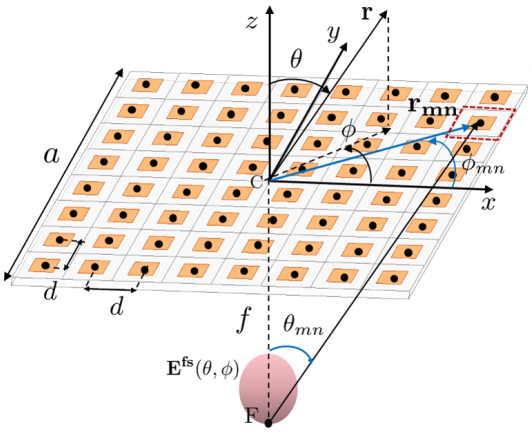


Fig. 1. Geometry of a transmitarray antenna and main parameters of the proposed model.

In this contribution, the model and phase-only synthesis approach based on iterative convex optimization preliminarily presented in [11] are revisited for centrosymmetric TAs. A convex formulation for the synthesis of a broadside beam with multiple constraints on the sidelobe levels (SLLs) and on the gain loss is proposed, leveraging on semidefinite relaxation [12]. A 20×20 TA fed by a 10-dBi horn is optimized to obtain very low SLLs in all azimuthal planes. A 3-bit TA approximating the optimal phase distribution is designed using the eight UCs reported in [5]. The antenna is fabricated using a standard printed circuit board (PCB) process and only three metal layers. The measurements experimentally demonstrate, for the first time, the robustness of the proposed synthesis method and design to realize focused-beam TAs at 300 GHz, despite the tolerances and constraints of PCB technology.

II. Model and Synthesis Procedure

We assume that the planar lens has $2N \times 2N$ elements, is symmetric about its center $C \equiv (0, 0, 0)$ and is illuminated by a feed whose phase center is in $F \equiv (0, 0, -f)$, where f is the focal distance, as shown in Fig. 1. The far-field feed

pattern is $\mathbf{E^{fs}}(\theta,\phi)$. The UCs are schematized as a pair of receiving (Rx) and transmitting (Tx) elements on the feed side and in the radiating medium, respectively, coupled by a phase shifter [3], [11]. The expression for the field $E^{inc}_{m,n}$ received by the mn-th TA element is given in [11]. It depends on the feed pattern and on the angle of view of each UC from the feed. In the synthesis, a perfect transmission from the Rx to the Tx elements of each UC is assumed. Thus, the transmission coefficient of the mn-th cell is $w_{m,n} = e^{j\angle w_{m,n}}$. The symmetry of the TA yields

$$\begin{aligned} w_{m,n} = w_{-m,n} = w_{m,-n} = w_{-m,-n}, \\ \text{for} \quad m = 1,\dots,N, \quad n = 1,\dots,N. \end{aligned} \tag{1}$$

For simplicity, we consider that the TA has the same period d along both x- and y-axis, so that the UCs are square. Similarly to [13], the Tx element of each UC is modeled as a radiating aperture of size $d \times d$, uniformly excited by a y-polarized field. Therefore, the far-field co-polar component of each Tx element can be written as

$$\begin{aligned} E^{Tx}_{co}(\theta,\phi) = (1+\cos\theta)\,\mathrm{sinc}\left(\frac{k_0 d}{2}u\right)\mathrm{sinc}\left(\frac{k_0 d}{2}v\right) \\ \times\left(\sin^2\phi\cos\theta + \cos^2\phi\right), \end{aligned} \tag{2}$$

where $k_0 = 2\pi/\lambda_0$ is the wavenumber, λ_0 is the wavelength in vacuum, $u = \sin\theta\cos\theta$ and $v = \sin\theta\cos\theta$. By neglecting the spillover and using (1), the following expression for the co-polar component of the TA far-field pattern is derived

$$\begin{aligned} E_{co}(\theta,\phi) = 4\sum_{m=1}^{N}\sum_{n=1}^{N} w_{m,n}E^{inc}_{m,n}\cos\frac{(2m-1)k_0 du}{2} \\ \times\cos\frac{(2n-1)k_0 dv}{2}E^{Tx}_{co}(\theta,\phi). \end{aligned} \tag{3}$$

The variation of $|E^{inc}|$ over the lens enforces the TA amplitude taper. Following the steps described in [12], the power pattern radiated by the TA is then expressed as

$$|E_{co}(\theta,\phi)|^2 = \mathrm{Tr}\left(\mathbf{A}(\theta,\phi)\,\mathbf{X}\right), \tag{4}$$

where $\mathbf{A} \in \mathbb{R}^{2N^2\times 2N^2}$ is a real symmetric matrix of known coefficients, $\mathbf{X} = \mathbf{x}\mathbf{x}^T$ is a rank-one semidefinite matrix of the same size, $\mathbf{x} = \left[\Re\{\mathbf{w}^T\}\ \Im\{\mathbf{w}^T\}\right]^T$ and $\mathbf{w}$ is the column vector of the N^2 unknown UC transmission coefficients to be optimized. The problem of synthesizing the TA to radiate a broadside beam with reduced SLLs by optimizing only the UC phase shifts ($\angle w_{m,n}$) is not convex. A semidefinite relaxation of this problem can be obtained by dropping the rank-one constraint on $\mathbf{X}$ and solved by iterative convex optimization [12]. At the i-th iteration, the convex synthesis problem is

$$\underset{\mathbf{X}}{\text{minimize}} \quad \mathrm{Tr}\left(\left(\mathbf{X}^{(i-1)} + \delta\mathbf{I}\right)^{-1}\mathbf{X}\right) \tag{5a}$$

subject to

$$\mathrm{Tr}\left(\mathbf{A_0}\mathbf{X}\right) \geq \gamma \max_{\mathbf{w}} |E_{co}(0^\circ,0^\circ)|^2, \tag{5b}$$

$$\mathrm{Tr}\left(\left(\mathbf{A}(\theta_p,\phi_q) - \rho_{p,q}\mathbf{A_0}\right)\mathbf{X}\right) \leq 0,\ \forall(\theta_p,\phi_q) \in S, \tag{5c}$$

$$\mathrm{Tr}\left(\mathbf{Q}_l\mathbf{X}\right) = 1, \quad l = 1,\dots,N^2, \tag{5d}$$

$$\mathbf{X} \succcurlyeq 0, \tag{5e}$$

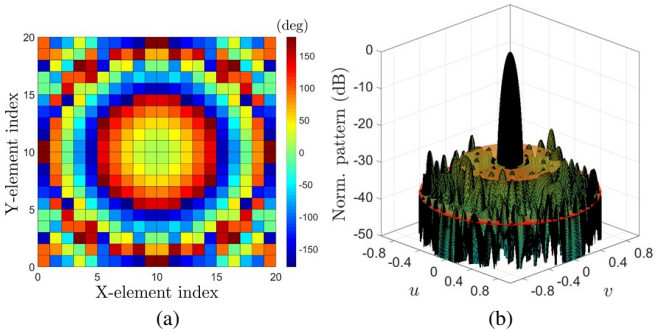


Fig. 2. (a) Phase distribution of the 20×20 synthesized TA. (b) Radiation pattern, calculated at 300 GHz using (3), and prescribed pattern envelope.

where $\mathbf{A_0} \triangleq \mathbf{A}(0^\circ,0^\circ)$. The objective function of (5) is based on the *log-det* heuristic [14] for rank minimization. The identity matrix is denoted by $\mathbf{I}$ and δ is a regularization factor. The first constraint enforces the broadside beam collimation and a maximum field intensity loss γ with respect to the maximum achievable value along the same direction, which is readily found from (4). The values of the power pattern in the sidelobe region S are prescribed in (5c), with respect to $|E_{co}(0^\circ,0^\circ)|^2$, using the factor $0 < \rho_{p,q} < 1$. The constraint on the unitary magnitude of the UC transmission coefficients is expressed by (5d). The N^2 diagonal matrices $\mathbf{Q}_l \in \mathbb{R}^{2N^2\times 2N^2}$ are defined in [12]. Finally, the constraint (5e) ensures that the solution is a positive semidefinite matrix.

The rank-one approximation $\mathbf{X}^{(i)}$ of the solution $\mathbf{X}^*$ of the convex problem at the i-th iteration is used for the next iteration. It is obtained by retaining only the largest eigenvalue of $\mathbf{X}^*$ [12]. The identity matrix is chosen as initial guess of the iterative synthesis: $\mathbf{X}^{(0)} = \mathbf{I}$.

III. Synthesis Results

A 20×20 broadside TA is synthesized after fixing its illumination, by solving problem (5). The TA period is $0.5\,\lambda_0$, so that its edge $a = 10\lambda_0$. The feed is a 10-dBi standard gain horn, at distance $f = 7.5$ mm from the planar lens ($f/a = 0.75$). It is modeled by using its simulated far-field radiation pattern at 300 GHz. The sidelobe region S is defined as:

$$\begin{aligned} S &= S_1 \cup S_2, \\ S_1 &= \{(\theta,\phi)\,|\,10^\circ \leq |\theta| \leq 34^\circ,\ 0^\circ \leq \phi < 180^\circ\}, \\ S_2 &= \{(\theta,\phi)\,|\,45^\circ \leq |\theta| \leq 90^\circ,\ 0^\circ \leq \phi < 180^\circ\}. \end{aligned} \tag{6}$$

The prescribed maximum SLLs are -30 dB in S_1 and -38 dB in S_2, respectively. Moreover, the value $\gamma = 0.7$ is set so that the gain loss, with respect to the maximum achievable value, does not exceed 1.5 dB. At each iteration, the problem (5) is solved using the Matlab-based software for convex optimization CVX [15]. The synthesized TA phase distribution is shown in Fig. 2a. It has been obtained considering that any phase value can be realized. The phase over each UC is assumed uniform. The corresponding three-dimensional radiation pattern is computed at 300 GHz by using the TA

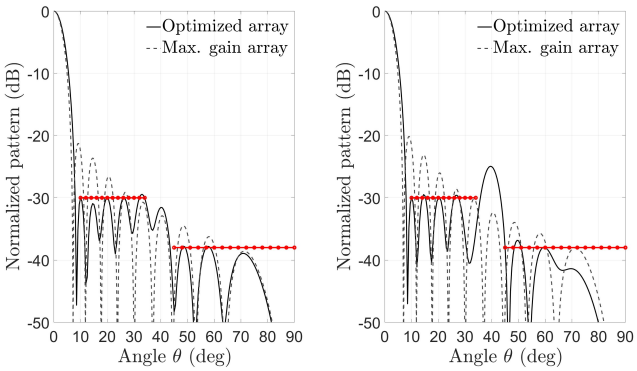


Fig. 3. Radiation patterns of the synthesized TA and of the corresponding TA optimized for maximizing the broadside gain. Results for (a) $\phi = 0°$ and (b) $\phi = 90°$.

model discussed in Section II and plotted in Fig. 2b. The desired mask is overlaid on the same plot. The constraints on the SLLs are met for all points where the mask has been numerically defined. The cuts of the radiation pattern in the principal planes and the prescribed masks (in red), are shown in Fig. 3. They are compared to the patterns calculated using the same model when the TA phase is optimized for maximizing the broadside gain. The patterns are normalized to their respective broadside values and are plotted for non-negative values of θ, by virtue of symmetry. It can be observed that the TA synthesis reduced of 10 dB and 8 dB the first SLL in the plane $\phi = 0°$ and $\phi = 90°$, respectively. The computed gain for the synthesized TA is 26.5 dB, which is 1.4 dB lower than the maximum achievable value for the same illumination.

IV. Prototype Design and Characterization

A 20×20 prototype is designed using the eight UCs presented in [5]. The size of all UCs is $\lambda_0/2 \times \lambda_0/2$ at 300 GHz. The phase shifts that they introduce achieve an almost uniform 3-bit quantization of the 360° range. The TA is designed by selecting, element by element, the UC providing the closest phase shift to the optimal value determined by the synthesis procedure (see Fig. 2a). Table I reports the magnitude and phase of the transmission coefficients of the eight UCs. These values were obtained from full-wave simulations of the UCs, performed in Ansys Electronics 2020, under normal incidence and using periodic boundary conditions.

The radiation pattern of the designed 3-bit TA is computed plugging in (3) the simulated transmission coefficients of the UCs. The pattern cuts in the principal planes are shown in Fig. 4 along with the results of a full-wave simulation of the whole TA, which was run using a hybrid solver based on finite element method and integral equation. The computed patterns, shown in solid lines, still approach the prescribed mask, but slightly exceed the SLL constraints in some points. The normalized pattern reaches -27 dB in S_1 and -35 dB in S_2. This is essentially due to the phase errors introduced by

TABLE I
Simulated Transmission Coefficients of the UCs

Cell	Magnitude (dB)	Phase (deg)
1	-0.70	-2.0
2	-0.44	49.0
3	-0.51	85.5
4	-0.51	139.8
5	-0.74	177.8
6	-0.47	230.0
7	-0.52	265.3
8	-0.55	318.4

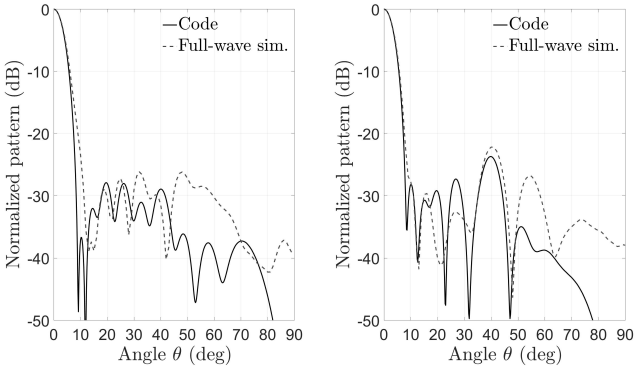


Fig. 4. Radiation patterns of the synthesized 3-bit TA obtained using the numerical model and a full-wave solver. Results for: (a) $\phi = 0°$ and (b) $\phi = 90°$.

the 3-bit quantization and, secondarily, to the small amplitude imbalance determined by the different insertion losses of the UCs. The simulated results (dashed lines) are in good agreement with the numerical ones in S_1. However, the simulated SLLs in the region S_2 are higher than those predicted by the code, even if still lower than -27 dB. The observed discrepancies are mainly due to the simplifying assumptions the TA proposed model relies on. In particular, the impact of spillover on the radiation patterns is not considered and the transmission coefficients of the UC are assumed independent of the angle of incidence of the impinging wave. Moreover, the non-periodicity of the TA is not taken into account, i.e. the coupling among different types of UCs is not modeled.

The prototype was fabricated using a low-cost PCB process, with minimum design features of 80 μm. The stack-up comprises two dielectric substrates, a bonding film and three metal layers. The overall thickness of the flat lens is about 0.29 mm No vias are employed. The PCB and the horn feed are assembled using plastic spacers on the TA edges (see Fig. 5). The antenna is characterized in reception in an anechoic chamber at CEA-Leti, using a 20-dBi horn as transmitting antenna and millimeter-wave vector network analyzer (VNA) extenders. The measured normalized pattern at 300 GHz (plane $\phi = 0°$) is compared to the simulated one

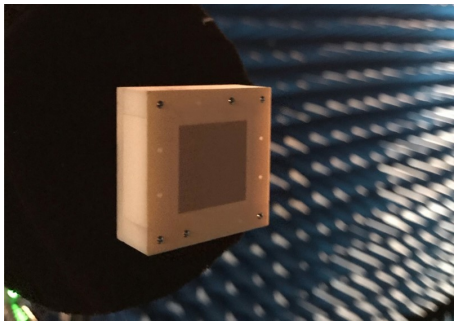


Fig. 5. Picture of the 3-bit TA under test in the anechoic chamber.

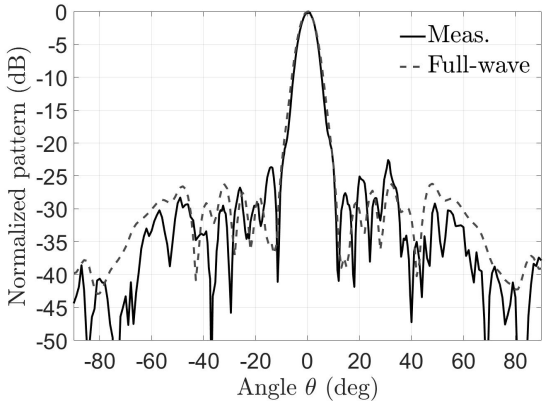


Fig. 6. Measured and simulated radiation patterns ($\phi = 0°$) of the 3-bit TA prototype at 300 GHz.

in Fig. 6. The beamwidth of the main lobe, the roll-off and the overall level of the sidelobes are well predicted. Some differences, such as the higher level of first sidelobes, can be attributed to the fabrication tolerances, alignment errors, and to the impact of the mechanical supports of the antenna which were not included in simulations.

V. Conclusion

A mathematical framework for the phase-only synthesis of symmetric focused-beam TAs with reduced SLLs has been presented. The TA phase distribution is found using an iterative procedure based on semidefinite relaxation which, at each step, optimally solves a convex sub-problem. A 400-element TA has been successfully synthesized to meet multiple challenging constraints on the SLLs in all azimuthal cuts of the radiation pattern and minimize the gain loss (1.4 dB) with respect to the maximum achievable value. Using the optimized phase and a set of eight UCs, a 3-bit prototype is designed at 300 GHz. By comparison with full-wave simulations, it has been assessed that the phase quantization introduces minor distortion on the far-field pattern. The flat lens has been fabricated using a low-cost three-layer PCB without vias. The measurements prove the effectiveness of the synthesis procedure in reducing the level of the first sidelobe levels (between -25 dB and -30 dB) and the robustness of the design to fabrication and mechanical tolerances. In future works, the TA model could be augmented by removing some simplifying assumptions, such as neglecting the impact of the spillover radiation, to improve the performance of the synthesis for large elevation angles.

Acknowledgment

This work was partly supported by the French Agency for National Research (ANR) through the project "Next5G" under Grant ANR 18-CEA25-0009-01.

References

[1] Y. Xing and T. S. Rappaport, "Terahertz wireless communications: cosharing for terrestrial and satellite systems above 100 GHz," *IEEE Comm. Lett.*, vol. 25, no. 10, pp. 3156–3160, Oct. 2021.

[2] K. Konstantinidis et *et al.*, "Low-THz dielectric lens antenna with integrated waveguide feed," *IEEE Trans. Terahertz Sci. Tech.*, vol. 7, no. 5, pp. 572–581, July 2017.

[3] J. R. Reis, M. Vala, and R. Caldeirinha, "Review paper on transmitarray antennas," *IEEE Access*, vol. 7, pp. 94 171–94 188, 2019.

[4] Z. W. Miao *et al.*, "140 GHz high-gain LTCC-integrated transmit-array antenna using a wideband SIW aperture-coupling phase delay structure," *IEEE Trans. Antennas Propag.*, vol. 66, no. 1, pp. 182–190, Jan. 2018.

[5] O. Koutsos, F. Foglia Manzillo, A. Clemente, and R. Sauleau, "Design of a 3-bit transmitarray antenna at 300 GHz using asymmetric linear polarizers," in *Proc. IEEE Antennas Propag. Soc. Int. Symp.*, 2020, pp. 1505–1506.

[6] N. Gagnon, A. Petosa, and D. A. McNamara, "Research and development on phase-shifting surfaces (PSSs)," *IEEE Antennas Propag. Mag.*, vol. 55, no. 2, pp. 29–48, Feb. 2013.

[7] F. Diaby, A. Clemente, K. T. Pham, R. Sauleau, and L. Dussopt, "Circularly polarized transmitarray antennas at Ka-band," *IEEE Antennas Wirel. Propag. Lett.*, vol. 17, no. 7, pp. 1204–1208, 2018.

[8] A. H. Abdelrahman, P. Nayeri, A. Z. Elsherbeni, and F. Yang, "Single-feed quad-beam transmitarray antenna design," *IEEE Trans. Antennas Propag.*, vol. 64, no. 3, pp. 953–959, Mar. 2016.

[9] H. Nematollahi, J. Laurin, M. Barba, and J. A. Encinar, "Realization of focused beam and shaped beam transmitarrays based on broadband unit cells," *IEEE Trans. Antennas Propag.*, vol. 65, no. 8, pp. 4368–4373, Aug. 2017.

[10] G.-B. Wu, K. F. Chan, and C. H. Chan, "3-D printed terahertz lens to generate higher order Bessel beams carrying OAM," *IEEE Trans. Antennas Propag.*, vol. 69, no. 6, pp. 3399–3408, June 2021.

[11] F. Foglia Manzillo, M. Śmierzchalski, N. di Pietro, A. Clemente, and M. Merluzzi, "Synthesis of transmitarrays via convex relaxation," in *Proc. IEEE Antennas Propag. Soc. Int. Symp.*, 2020, pp. 2017–2018.

[12] B. Fuchs, "Application of convex relaxation to array synthesis problems," *IEEE Trans. Antennas Propag.*, vol. 62, no. 2, pp. 634–640, Feb. 2014.

[13] E. G. Plaza, G. León, S. Loredo, and F. Las-Heras, "A simple model for analyzing transmitarray lenses," *IEEE Antennas Propag. Mag.*, vol. 57, no. 2, pp. 131–144, Apr. 2015.

[14] M. Fazel, H. Hindi, and S. Boyd, "Rank minimization and applications in system theory," in *Proc. Amer. Contr. Conf.*, vol. 4, 2004, pp. 3273–3278.

[15] M. Grant and S. Boyd, "CVX: Matlab software for disciplined convex programming, version 2.1," http://cvxr.com/cvx, Mar. 2014.